Effect of Process Parameters and Heat Treatment on the Microstructure and Mechanical Properties of SLM-built HY100 steel

J.J.S. Dilip*, Brent Stucker * and Thomas L. Starr**

*Department of Industrial Engineering, **Department of Chemical Engineering,
J.B. Speed School of Engineering, University of Louisville, Louisville, KY 40292

REVIEWED

Abstract

HY100 is a high strength low alloy steel used for naval and pressure vessel applications. In general, the alloy is used in the quenched and tempered condition. In the present work, fully dense metallic samples were produced from HY100 pre-alloyed powders using selective laser melting (SLM). Test samples were built with varying process parameters (scan speed and laser power). The SLM-built samples were given direct tempering treatment and a standard quench and temper heat treatment. Tensile properties of the samples were evaluated in direct temper, and quench and temper conditions. The study investigates the influence of process parameters and heat treatment on the microstructure and mechanical properties of SLM-built HY100 steel.

Introduction

Additive manufacturing involves layer-by-layer fabrication of a three-dimensional part based on computer-aided design data. It involves mathematically slicing a CAD model of the part to be produced into a number of horizontal layers and systematically creating these layers one over another, from bottom to top, to produce the part. There are a number of commercially available additive manufacturing processes such as Laser Engineered Net Shaping (LENS), Selective Laser Melting (SLM), and Electron Beam Melting (EBM), which can produce complex-shaped end-use metallic parts [1]. In all these processes material addition is achieved through melting and solidification.

Selective Laser Melting (SLM) is a powder bed fusion-based additive manufacturing process in which successive layers of metal powder particles are melted and solidified on top of each other by a high intensity laser beam [2]. SLM of materials is generally accompanied with high cooling rates due to the short dwell time and high thermal gradients. These high cooling rates during SLM may result in the formation of finer microstructural features when compared to traditional manufacturing methods [2,3]. The process of layer-by-layer deposition causes each deposited layer to experience multiple thermal cycles during the build which in-turn can result in varied microstructures. Microstructures are governed by the processing parameters and in turn, control the part mechanical properties [3,4].

In the present study, HY100 pre-alloyed powders were used to produce 3D metallic parts using SLM. The alloy usually gains its required properties by heat treatment, which initially involve austenitizing at high temperature and quenching to form fully martensitic microstructures (hard and brittle). The high hardness of quenched martensite is mainly due to high carbon concentration in the lattice of martensite [5]. To obtain acceptable levels of ductility and toughness, the alloy is subjected to tempering. Isothermal holding at the tempering temperature causes the carbon in the martensite lattice to precipitate out as carbide particles within the martensite phase. The formation of these carbides results in significant reduction in hardness and improved ductility and toughness with an acceptable loss in yield strength [6]. The final microstructure after quench-and-temper condition consists of tempered martensite and/ or bainite phases [7]. The microstructure is tuned such that it gives a high yield strength (690 MPa, min.) while maintaining good toughness and ductility [8].

Essentially no information is available on SLM of HY100 steel in the open literature. Microstructure evolution in this steel during SLM can be complicated because of the multiple thermal cycling effects. Hence, the parts in as-built condition may develop some microstructure-property problems. Therefore, it may be necessary to employ a suitable heat treatment for achieving satisfactory part mechanical properties. The objectives of the present work are:

(i) Optimization of the processing parameters to produce fully dense metallic samples from HY100 pre-alloyed powders.
(ii) Studies on mechanical properties of the HY100 SLM samples in various heat treatment conditions.

Experimental methods

Gas atomized HY100 pre-alloy steel powder (Sandvik Osprey) were used in the present study. The nominal composition of the HY100 powders is presented in Table 1. The powder particle size and distribution were measured using a Microtrac S3000 particle size analyzer. Further, SEM observations for the size and morphology of the powders were also performed.

Table 1. Chemical composition of HY100 steel powders

Element	C	Ni	Cr	Mo	P	S	Mn	Si	V	Ti	Cu	Fe
wt.%	0.1-0.22	2.6-3.5	1.29-1.86	0.27-0.63	0.02 max.	0.02 max.	0.1-0.45	0.12-0.38	0.03	0.02	0.25	Bal.

The processing of HY100 powder involves two steps: fabrication in the SLM machine and post-build thermal treatment. Samples were produced using an EOS M270 Direct Metal Laser Sintering (DMLS) machine in a nitrogen purging atmosphere. The protective gas allows maintaining the oxygen content to low levels to prevent the oxidation of HY100 powders during part fabrication. Initially, small cubes (10 mm X 10 mm X 10 mm) were fabricated using several parameter sets in order to study the effect of processing parameters on the density of SLM-processed parts and to select "optimal" parameters to fabricate tensile specimens. Seven parameter sets were created by varying laser power, scan speed and scan offset distance. The combination of parameters was constrained to three energy densities. The parameters used are listed in table 2.

Table 2. Process parameters for fabricating HY100 steel samples.

Parameters #	Laser Power (W)	Hatch Distance (μm)	Speed (mm/s)	Layer thickness (μm)	Energy density (J/mm^3)
1	195	100	833	40	58
2	195	120	700	40	58
3	175	100	750	40	58
4	195	120	765	40	53
5	195	100	920	40	53
6	195	120	625	40	65
7	195	100	750	40	65

A mild steel plate with dimensions 300 mm × 300 mm × 25 mm was used as the build platform. Flat tensile specimens (ASTM E-8) were fabricated using the optimal parameter set. Fig.1 shows the base plate with the tensile samples and small cubes. As can be seen from Fig.1, the samples were not precisely oriented along the x and y axes, so throughout the rest of this paper the samples that were most nearly aligned with the x and y axes are labeled XZ and YZ build orientations respectively. These builds were used for carrying out various heat treatments (Table 3) and tensile tests.

Microstructural characterization was carried out on the as-built samples and on the heat treated samples. The samples were sectioned using a low speed saw. The cut samples were mounted in resin and polished using SiC sandpaper. Final polishing was carried out using 1 μm diamond suspension. The samples were etched using 4% Nital reagent. The cross-sectional microstructure of the unetched and etched conditions were examined by optical microscopy (OM) and SEM. Rockwell hardness measurements were carried out on the as-built and heat treated samples. The reported values are the average of five indentations measured on the sample. Hardness results are presented in table 3.

Tensile tests were carried out for specimens fabricated in XZ and YZ orientations with as-built and heat treated tensile samples. The tensile test results such as yield strength, ultimate tensile strength, and percentage strain-to-failure were reported. The percentage strain-to-failure was measured using an extensometer clipped to the gage section of the test specimen. Fracture surface examination of the tensile tested samples was also performed using SEM.

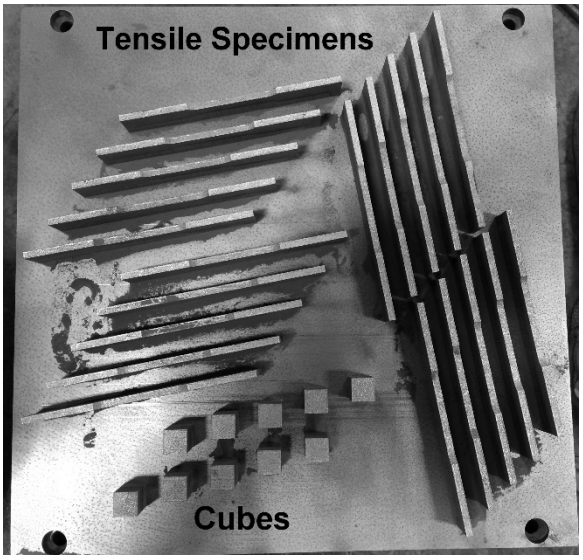

Fig. 1 Photograph showing a build plate with flat tensile samples (YZ) and small cubes

Results and Discussion

Fig.2 a & b show the morphology of the powder particles. The diameters of individual particles were measured from several different SEM micrographs to estimate the size and distribution of the particles. It was estimated that particles have a size distribution between 5 μm and 40 μm. The powders were spherical in shape, which is an important powder characteristic for good flowability. A good flowability is necessary for better powder layer deposition and also ensures that the powders can be dispensed properly [9]. SEM shows typical dendritic morphology features on the surface of the particles. The larger particles were observed to have satellite particles attached. These small particles form due to

fragment micro droplets sticking to the larger particles. The mean particle diameter is ~30 μm with a standard deviation of 10 μm as measured by particle size analysis. The results from particle size analysis show a bi-modal distribution of the powder particles (Fig.2b).

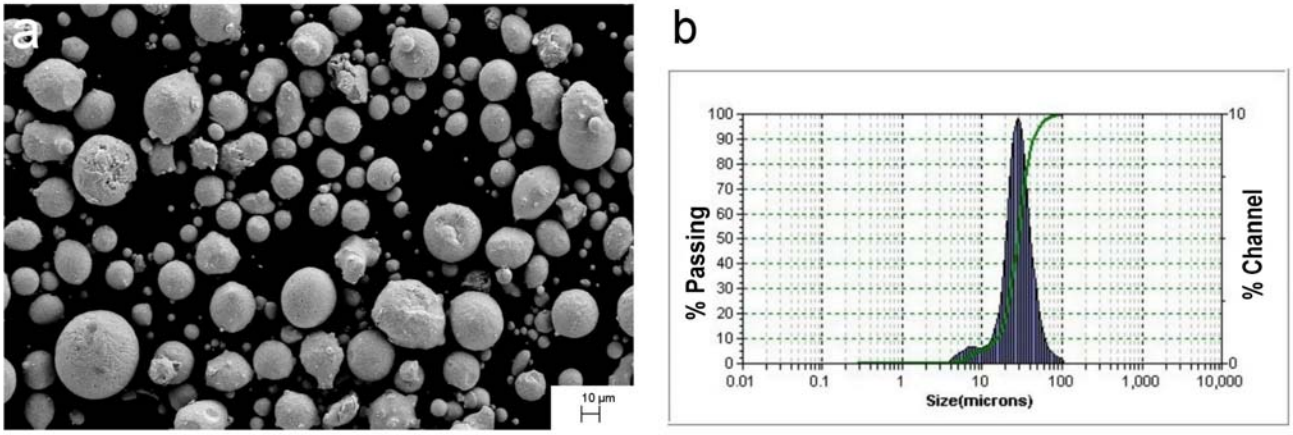

Fig. 2 (a) Scanning electron micrographs of the HY100 powders (b) Particle size distribution plot

For porosity measurement the cubes were metallographically prepared and examined in a polished condition using optical microscopy. Porosity in the sample was quantified using image analysis software. Fig.3 shows typical cross-section microstructures of SLM built cubes with different processing parameters. The dark irregular regions in the micrographs are pores (dark arrow) (Fig.3a). For each value of energy density, the porosity was not significantly different for different scan speed, power and distance parameters – at least within the range of values used. The deposits produced using an energy density of less than 60 J/mm^3 showed some porosity (1-2%), but those produced at higher energy densities were fully dense (Fig.3b). All SLM built HY 100 samples contained very fine non-metallic oxide particles in the matrix (fine dark spots in the micrograph Fig.3b). After these series of experiments were performed to establish suitable parameters for fully dense parts, processing parameter combination # 6 was used for further study.

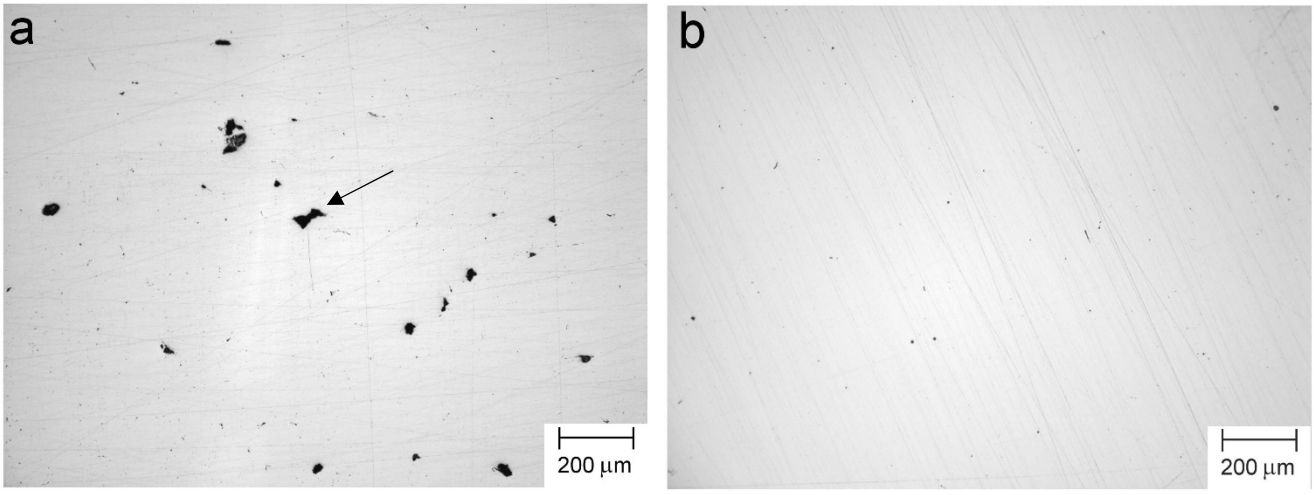

Fig. 3 Typical cross-sectional micrograph of an as polished sample (a) with significant amount of porosity (parameter set #5) (b) fully dense (parameter set #6)

Energy density is an important factor that affects the properties of as-built parts fabricated by SLM processing. The energy density E (J/mm^3) in SLM is expressed in equation (1), where P is laser power (W), v is scan speed (mm/s), h is hatch spacing (mm) and t is layer thickness (mm) [10].

$$E = P / v*h*t \quad (1)$$

Energy density directly indicates the energy input into to the process (ignoring any base plate or other bulk heating). A higher laser power provides more energy density for good melting and spreading of the melt pool. However, fusion defects or porosity can result if the scan speed is too high for a given laser power (due to insufficient laser-material interaction time). Similarly, too high a hatch spacing can cause fusion defects between individual scan lines or tracks. It should be noted that scan speed, hatch spacing and laser power are mutually dependent and are to be optimized considering their combined effects during SLM [11]. In the present study, the parameters with higher energy density appear to be near-optimum for producing fully dense samples from HY100.

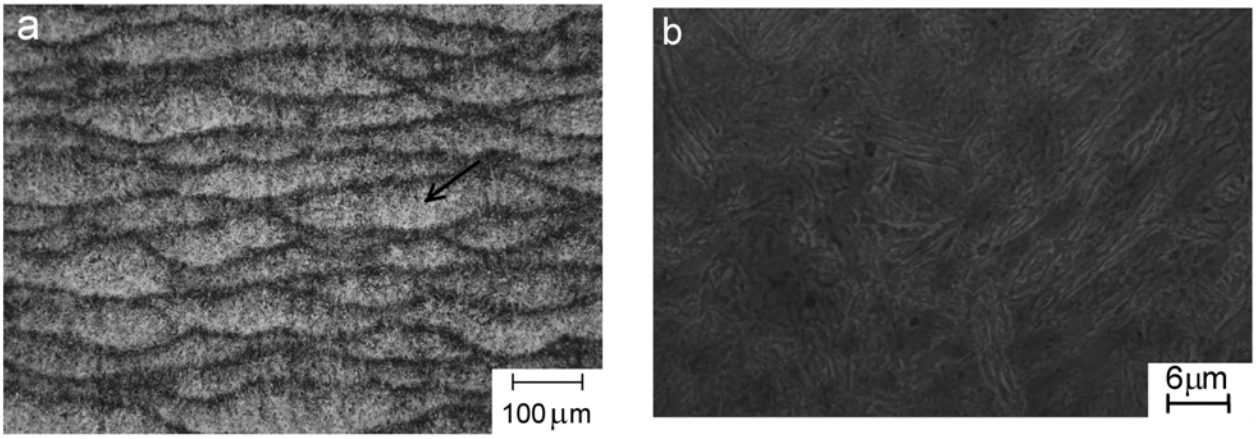

Fig. 4 Micrographs of an as-built fully dense HY100 steel sample (a) Optical and (b) SEM.

An optical micrograph of a vertical cross-section of a fully dense SLM fabricated cube sample is presented in Fig.4a. The micrograph shows multiple layers clearly delineated by the dark etch bands along the fusion boundaries. During SLM the powders are exposed to high intensity laser energy, which causes the powder temperature to rise above the melting point. As the laser passes away the molten pool of metal solidifies along the line of laser scan. The laser beam also causes partial melting of the below/adjacent layers, thereby allowing fusion welding of the layers. The alloy HY100 initially solidifies as delta ferrite directly from the liquid phase and subsequently transforms to austenite. From the continuous cooling transformation curve of the alloy, the high temperature austenite transforms to martensite as the cooling rates experienced in the process are steep [7]. The solidified track of alloy will now consist of untempered martensite. The reported Ms and Mf temperatures for the alloy are much higher than room temperature. It is well-established that Ms temperature determines the microstructure and substructure formed during fast cooling. In the present alloy, lath martensite is expected to form due to higher Ms temperature [5]. Fig.4b (region indicated by arrow in Fig.4a) shows a high magnification SEM micrograph of the as deposited sample revealing lath morphology of martensite.

Since the part fabrication takes place by layer-by-layer melting and solidification of the powders, the deposited layers underneath experience complex multiple thermal cycling effects. This scenario is equivalent to multi-pass welding of the material. Hence, it can be anticipated that during layer-wise

deposition, the regions which are reheated to high enough temperatures can experience martensite tempering [12]. However, in the present situation the thermal cycles are very brief, which can result in partial or slight tempering of martensite. In other words, it is quite unlikely that complete tempering of martensite would result during laser processing. Hence, the part in the as-built condition is unsuitable for direct application due to the hard untempered martensitic microstructure. Also, laser deposited parts are prone to residual stress accumulation during the process [13]. Thus, it is essential to determine proper heat treatments for achieving desired part mechanical properties.

The as-built cubes were subjected to different heat treatments and Rockwell hardness tests (Table 3). In one set of experiments the as-built cubes were given direct tempering and in another set, initial stress relief followed by full heat treatment (by austenize and quench, and then tempering). The stress relieving treatment was carried out at a maximum temperature of 600ºC for 1 hour. Table 3 summarizes the overall heat treatment effects on hardness.

The MIL-S-16216 standard specification emphasizes an austenizing temperature of 900ºC for 1 hour followed by a quenching and tempering temperature not less than ~620ºC for HY100.The MIL standard leaves selection of tempering temperature to the manufacturer for meeting the desired mechanical properties [8]. It is well known from literature that tempering causes reduction in hardness of martensite due to the removal of carbon from the martensite lattice. The carbon reacts with Fe, Cr, and Mo and forms carbides within the martensite phase. The removal of carbon and formation of carbide particles will generally result in improved toughness / ductility with an acceptable loss in strength and hardness. This quench and temper process creates a tempered martensitic structure. The hardness measurements show reduction in hardness due to tempering of martensite. As expected, the hardness of the heat treated samples was influenced by the tempering temperature. It was quite interesting to note that the hardness of the direct temper and full heat treatment samples did not show large differences. The hardness of the as-built sample was similar to the direct quench sample, which further confirms that during multilayer deposition tempering of martensite has no considerable effect.

Table 3. List of heat treatments carried out on SLM HY100 samples and their corresponding hardness.

Heat treatment	HRc (avg. of 5 readings)
As-built HY 100	37
900ºC-1h-WQ*	38
Direct temper 620ºC-2h-AC**	26
900ºC-1h-WQ* + 620ºC-2h-AC**	21
Direct temper 650ºC-2h-AC**	22
900ºC-1h-WQ* + 650ºC-2h-AC**	22
Direct temper 670ºC-2h-AC**	20
900ºC-1h-WQ* + 670ºC-2h-AC**	18

*WQ : Water Quench, ** AC : Air Cool

The heat treated samples were examined under SEM and micrographs are presented in Fig.5. The micrographs show tempered martensite and bainite. It was very difficult to deduce quantitative differences in microstructures between the direct and fully heat treated samples. Nevertheless, high temperature tempered samples (670ºC) show coarser microstructural features. Further detailed higher

magnification studies by TEM are necessary in order to fully understand the nature of carbides, their size and distribution in the microstructure and their effects on mechanical properties.

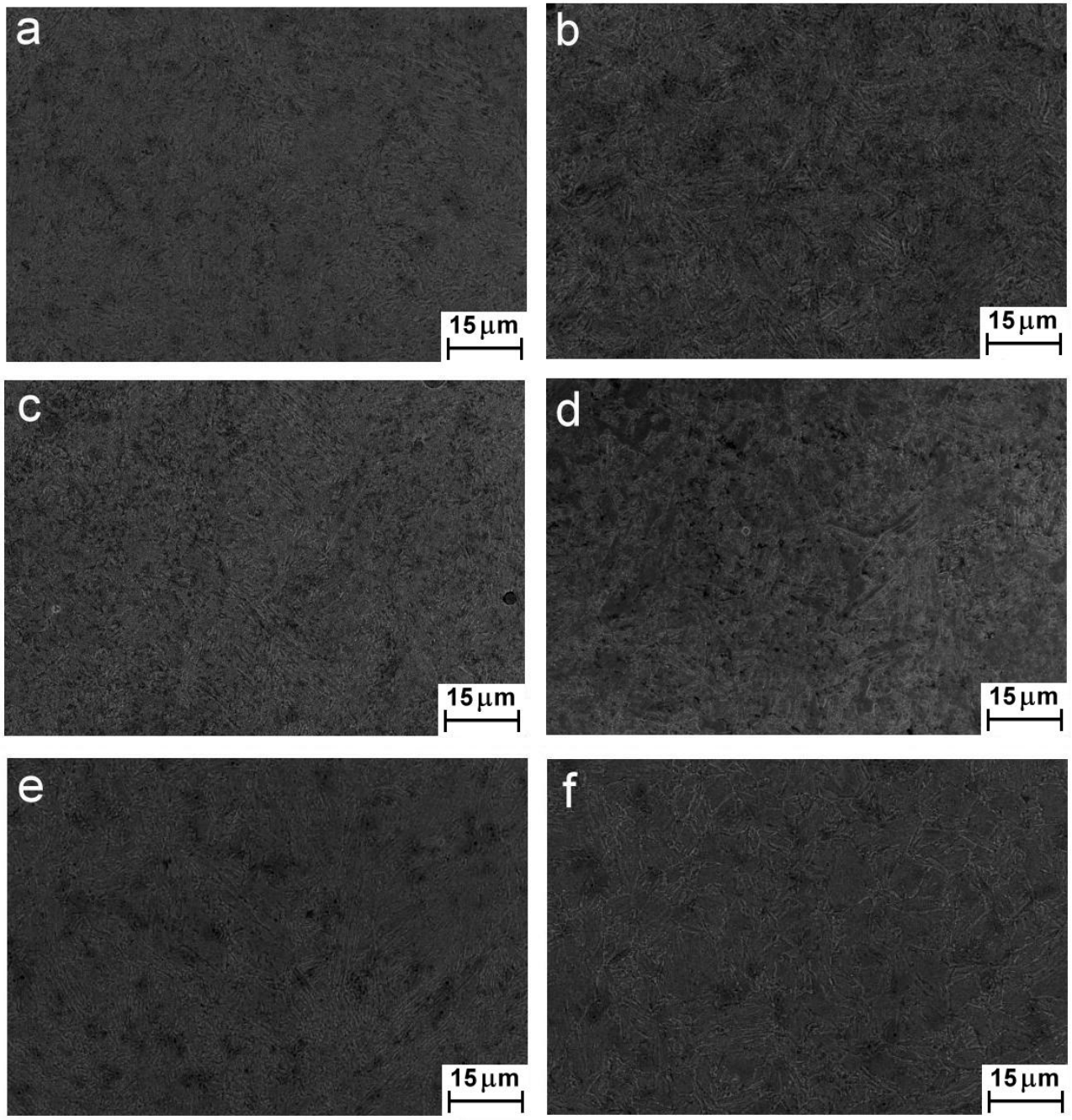

Fig. 5 SEM micrographs of HY100 steel in different heat treatment conditions (a) Direct temper at 620ºC (b) Quench-and-temper at 620ºC (c) Direct temper at 650ºC (d) Quench-and-temper at 650ºC (e) Direct temper at 670ºC (f) Quench-and-temper at 670ºC.

It is well agreed and documented that hardness bears a direct correlation to the strength of material [14]. A reduction in hardness indicates softening of martensite and also the degree of tempering. Therefore, heat treatments on tensile samples were carried out using direct temper and full heat

treatment. Three different tempering temperatures (620, 650 and 670ºC) were used. Tensile tests were carried out on the heat treated samples and results are given in Table 4.

Table. 4 Tensile test results for HY100 steel deposits in different heat treatment conditions.

Heat treatment	0.2 % Y.S (MPa)	UTS (MPa)	Strain to failure	Hardness HRc
As-built (YZ)	1172	1353	6	37
As-built (XZ)	1178	1325	4.5	--
Direct temper 620ºC-2h-AC	915	926	2.5	26
900ºC-1h-WQ + 620ºC-2h-AC	684	756	7	21
Direct temper 650ºC-2h-AC	750	880	4.5	22
900 ºC-1h-WQ + 650ºC-2h-AC	658	696	3.5	22
Direct temper 670ºC-2h-AC	704	886	7	20
900ºC-1h-WQ + 670ºC-2h-AC	586	750	7	18

The tensile test results show promising strength values in the heat treated specimens. The as deposited samples with different orientations showed similar mechanical properties. This was expected since the scan pattern variation in these samples should normalize properties in the XY plane. It is expected, however, that samples in the Z orientation may have differing mechanical properties. The heat treated samples showed a reduction in strength levels as the tempering temperature was increased. It was interesting to note that direct temper samples gave good yield strength values. Therefore, it can be deduced that HY100 steel SLM fabricated parts can be subjected to direct tempering, thus eliminating the austenizing and quenching steps. The ductility of the as-built and heat treated samples was quite limited. SEM fractography studies of the fracture surfaces revealed (Fig.6) typical dimple rupture failure mode with transgranular ductile failure in the direct tempered and fully heat treated deposits. The sizes of the dimples were observed to be fine and shallow in the fracture surfaces. The size and shape of the dimples indicate the formability of the material, and finer dimples indicate lower elongation values [15]. The elongation values obtained are somewhat less than for the MIL-S-16216 specification. The phenomenon of lower elongation than expected was reported by several researchers for various additively manufactured alloys [16,17,18]. At present, the reason for lower ductility in the present HY100 alloy made using SLM is not fully clear. However, lower ductility can be partly attributed to the presence of fine nonmetallic oxides (Fig.7) and contribution from secondary hardening by precipitation of Molybdenum carbide during tempering [5]. These oxides were confirmed from EDS analysis as complex oxides of Al, Si and Mn. The presence of fine oxide particles will have significant effect on fracture initiation and propagation during tensile testing [19].

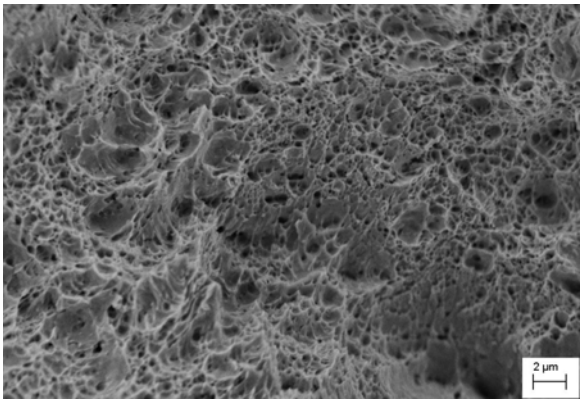

Fig. 6 SEM fracture surface of a direct tempered sample (650ºC-2h-AC). The fracture features exhibit a typical dimpled rupture mode of failure.

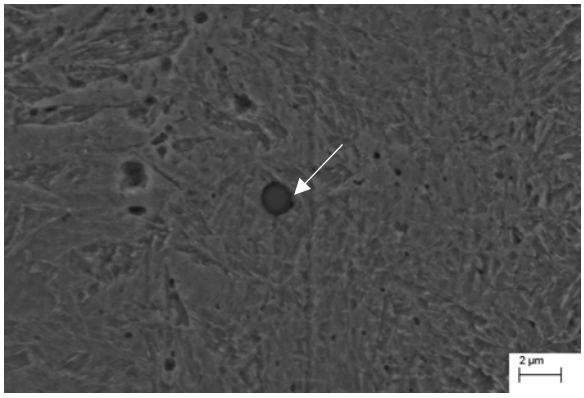

Fig. 7 SEM micrograph of the etched cross-section of the as-built, fully dense HY100 steel sample showing fine nonmetallic oxide particles.

Conclusions

In the current study, selective laser melting experiments were conducted using HY100 steel powders. Microstructural and mechanical properties of the HY100 SLM deposits were carried out. The following conclusions can be drawn from the present work:

- HY100 can processed using selective laser melting. Parameters for fully dense parts are possible.
- Thermal cycles involved in SLM have an effect on HY100 microstructural development, resulting in non-traditional microstructures. Suitable heat treatments are needed to achieve desired properties.
- HY100 components were subjected to direct tempering and full heat treatment involving austenize-quench and temper. Heat treatments were conducted at different tempering temperatures and were examined for microstructures and mechanical properties.
- The results from the tensile tests indicate that direct tempering of HY100 steel can provide good part mechanical properties, but with reduced ductility. A separate austenize /quench step can be eliminated when heat treating SLM HY100 parts. However, further experimental studies are recommended to fully understand a proper heat treatment schedule.

Acknowledgments

The authors gratefully acknowledge the support of the Tim Gornet, Mathew Taylor and Zach Daniel of the Rapid Prototyping Center at the University of Louisville for their help and assistance.

References

[1] I. Gibson, D.W. Rosen, B. Stucker, *Additive Manufacturing Technologies: Rapid Prototyping to Direct Digital Manufacturing*, Springer, New York, NY, 2009.

[2] K.Kempena, E.Yasa, L.Thijs, J.P. Kruth, J.Van Humbeeck, Microstructure and mechanical properties of Selective Laser Melted 18Ni-300 steel. *Physics Procedia* 12, 2011, 255–263.

[3] J.P. Kruth, L. Froyen, J. Van Vaerenbergh, P. Mercelis, M. Rombouts, B. Lauwers, Selective laser melting of iron-based powder, *Journal of Materials Processing Technology*, 149 (1–3), 2004, 616-622.

[4] Takayuki Nakamoto, Nobuhiko Shirakawa, Yoshio Miyata, Haruyuki Inui, Selective laser sintering of high carbon steel powders studied as a function of carbon content, *Journal of Materials Processing Technology*, 209 (15–16), 2009, 5653-5660.

[5] George E. Totten, Maurice A.H. Howes, Steel *Heat Treatment Handbook*, CRC Press 1997.

[6] John E. Holthaus, Michelle G. Koul, Angela L. Moran, Property and microstructure evaluation as a function of processing parameters: Large HY-80 steel casting for a US Navy submarine, *Engineering Failure Analysis* 13, 2006, 1397–1409.

[7] X. Yue, J. C. Lippold, B.T. Alexandrov, S.S.Babu, Continuous cooling transformation diagrams have been constructed for the coarse-grain heat-affected zone of HSLA-65, HSLA-100, and HY-100 steels,*Welding Journal*, 2012, 67s-75s.

[8] MIL-S-16216K(SH), Steel plate, alloy, structural, high yield strength (HY-80 and HY-100).

[9] Bochuan Liu, Ricky Wildman, Christopher Tuck, Ian Ashcroft, Richard Hague , Investigation the effect of particle size distribution on processing parameters optimisation in Selective Laser Melting process. *Solid Freeform Fabrication Symposium,* 2011, 227-238.

[10]Haijun Gong, Khalid Rafi, Thomas Starr, Brent Stucker, The Effects of Processing Parameters on Defect Regularity in Ti-6Al-4V Parts Fabricated By Selective Laser Melting and Electron Beam Melting, *Solid Freeform Fabrication Symposium,* 2013, 424-439.

[11] Hengfeng Gu, Haijun Gong, Deepankar Pal, Khalid Rafi, Thomas Starr, Brent Stucker, Influences of Energy Density on Porosity and Microstructure of Selective Laser Melted 17- 4PH Stainless Steel,*Solid Freeform Fabrication Symposium,* 2013, 474-489.

[12] P. Deb, K. D. Challenger,A. E. Therrien, Structure-property correlation of submerged-arc and gas-metal-arc weldments in HY-100 steel, *Metallurgical Transactions A* , 1987,Volume 18,Issue 13, 987-999.

[13] J.P. Kruth, L. Froyen, J. Van Vaerenbergh, P. Mercelis, M. Rombouts, B. Lauwers, Selective laser melting of iron-based powder, *Journal of Materials Processing Technology*, Volume 149, Issues 1–3, 10 2004, 616-622.

[14] Joseph R. Davis, TensileTesting, ASM International,OH, 2004.

[15] Lothar Engel, Herman Klinge, An Atlas of Metal Damage, Prentice Hall, Englewood Cliffs, New Jersey, 1981.

[16] Bo Song, Shujuan Dong, Sihao Deng, Hanlin Liao, Christian Coddet, Microstructure and tensile properties of iron parts fabricated by selective laser melting, *Optics & Laser Technology* 56 ,2014, 451–460.

[17] Bey Vrancken, Lore Thijs, Jean-Pierre Kruth, Jan Van Humbeeck, Heat treatment of Ti6Al4V produced by Selective Laser Melting: Microstructure and mechanical properties, Journal of Alloys and Compounds, 541(15), 2012,177-185.

[18]Xiaoming Zhao, Jing Chen, Xin Lin, Weidong Huang, Study on microstructure and mechanical properties of laser rapid forming Inconel 718, Materials Science and Engineering: A, 478(1–2), 2008, 119-124.

[19] D.N. Shackelton, Welding of HY 100 and HY 130 steels, A literature review, The Welding Institute, Cambridge, 1973.